Removal of Spurious Reflections from Computational Fluid Dynamic Solutions with the Complex Cepstrum

Kristine R. Meadows* and Jay C. Hardin†
NASA Langley Research Center, Hampton, Virginia 23665

The complex cepstrum is shown to remove spurious reflections from artificial boundaries in computational fluid dynamic (CFD) solutions. First, the complex cepstrum theory is presented. A time sequence consisting of a direct signal and reflections is analyzed theoretically with the complex cepstrum, and it is shown that the direct signal uncontaminated by reflections may be recovered in the time domain. Next, the complex cepstrum is applied to one- and three-dimensional CFD solutions, and spurious reflections from the boundary conditions are removed. By eliminating spurious reflections introduced by artificial boundary conditions, the applicability of CFD methods to aeroacoustic problems is enhanced greatly.

Introduction

COMPUTATIONAL fluid dynamics (CFD) has been used successfully in recent years to predict the aerodynamic performance of aircraft. If the aeroacoustician wishes to take full advantage of the computational tools available, then the application of CFD technology to the prediction of acoustic loads and noise radiation must be considered. There are obstacles to be overcome, however, before current CFD methods may be applied to aeroacoustic problems. One such problem is development and implementation of appropriate boundary conditions. Many problems of aeroacoustics are physically posed in an essentially infinite domain. The noise generated in a jet or helicopter, for instance, typically propagates long distances before interaction with the ground or other surfaces. However, the solution to this problem on a computer must obviously be constrained within a finite region. Artificial boundaries must be placed on the problem to make it finite.

When artificial boundary conditions reflect acoustic or mean flow information back into the solution domain, error and numerical stability problems may be introduced. Even when numerical stability is maintained, there are pathological cases in which the computed flowfield in the presence of small reflections is completely incorrect. Marginally stable flows such as the initial formation region of a turbulent jet or the transition region of a boundary layer, for instance, can be dramatically altered by the introduction of sound waves.

To avoid these difficulties, artificial boundaries are typically placed far enough away from the region of interest so that reflections from the boundary conditions will not adversely effect the solution. But this is done at the expense of computer time required to obtain the solution in large computational domains and is limited to short time solutions. Much research has been devoted to the development of nonreflecting boundary conditions.[1-3] However, the success of such boundary conditions seems to be limited. In fact, the development of perfectly nonreflecting local boundary conditions is not thought possible for unsteady multidimensional flows.[1]

The work described in this paper focuses on a novel approach to the problem of reflecting boundary conditions. The approach taken is to accept the fact that the boundary conditions will reflect, but to remove the reflections from the solution with a nonlinear digital signal processing technique called the complex cepstrum. By eliminating spurious reflections induced by artificial boundary conditions, the applicability of CFD methods to aeroacoustic problems is enhanced greatly.

Cepstrum analysis was introduced by Bogert et al.[4] in 1963 as a method for finding arrival times in composite signals and was given further impetus in the publication by Oppenheim et al.,[5] which introduced the complex cepstrum. Cepstrum analysis has been successfully applied to detect echoes in wind tunnel, seismic, geophysical, and gear-noise data. The benefits and limitations of applying the cepstrum method to experimental data are widely known. Childers et al.[6] include an exhaustive list of references on basic cepstrum theory and applications. The theses by Perraud,[7] Peardon,[8] Tavakolli,[9] and Meadows[10] also contain reviews of cepstrum applications. The application of cepstrum analysis techniques to numerical solutions is the topic of this paper.

Theory of the Complex Cepstrum

The complex cepstrum is defined[5] as the inverse Fourier transform of the complex natural logarithm of the Fourier transform of the time sequence $x(t)$,

$$C_c(\tau) = \int_{-\infty}^{\infty} \ell n[X(\omega)] e^{i\omega\tau}\, d\omega \qquad (1)$$

where τ is the independent variable of the complex cepstrum, and $X(\omega)$ is the Fourier transform of the time sequence $x(t)$.

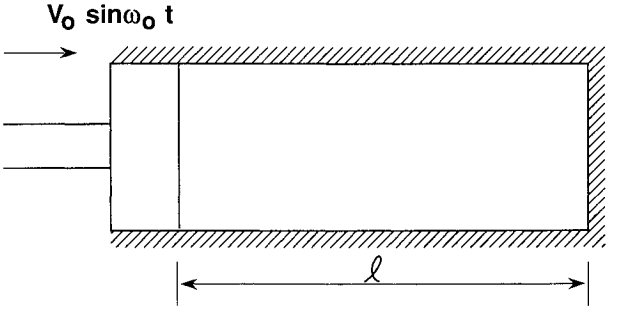

Fig. 1 Piston driving the velocity field in a duct.

Received Aug. 2, 1990; presented as Paper 90-3919 at the AIAA 13th Aeroacoustics Conference, Tallahassee, FL, Oct. 22-24, 1990; revision received Dec. 7, 1990; accepted for publication Jan. 28, 1991.

*Aerospace Engineer, Aeroacoustics Branch, Acoustics Division, Mail Stop 461.
†Senior Research Scientist, Aeroacoustics Branch, Acoustics Division.

It should be noted that, in the computation of the complex cepstrum, the first Fourier transform is followed by a nonlinear logarithmic process. Therefore, the inverse Fourier transform does not recover the original time domain. To avoid confusion, Bogert named the recovered domain the quefrency domain.[4] The independent variable is then called the quefrency. It is customary in the literature to use the units of time for quefrency since the original units are recovered when a Fourier transform is followed by the inverse Fourier transform.

The complex cepstrum preserves phase information because the logarithm is performed on the complex sequence $X(\omega)$. Hence, inverse complex cepstrum operations allow the original time signal to be recovered. This feature of the complex cepstrum makes it attractive for use with CFD solutions.

There are difficulties in applying complex cepstrum analysis, but remedies to these difficulties are available in the literature[4-13] and will not be reproduced here. The interested reader is referred to these papers for details.

Simple Model Problem

A simple example of a direct signal and single reflection will be used to demonstrate that the source signal and reflection are additively combined after taking the natural logarithm. The time history of a signal with a single reflection is modeled by the equation:

$$x(t) = s(t) + a_o s(t - t_o) \qquad |a_o| < 1 \tag{2}$$

where $s(t)$ is the original signal, and $a_o s(t - t_o)$ is the reflection of the original signal. Note that $s(t)$ in Eq. (2) may represent a signal propagating in a CFD solution. The reflection $a_o s(t - t_o)$ may represent the undesired reflection in the solution due to the presence of an artificial boundary in the computational domain. Although only a single reflection is considered here, the analysis may be extended to multiple reflections. Also note that the reflected signal(s) may overlap the original signal.

Performing the operations defined in Eq. (1) on the time history of Eq. (2) and using the infinite series expansion of $ln(1 + a_o e^{-i\omega t_o})$, the complex cepstrum of source signal and echo becomes,

$$C_c(\tau) = C_x(\tau) + 2\pi \sum_{n=1}^{+\infty} \frac{(-1)^{n+1}(a_o)^n}{n} \delta(\tau - nt_o) \tag{3}$$

where $C_x(\tau)$ is the complex cepstrum of the original signal $s(t)$, and $\delta(\tau - nt_o)$ is the Dirac delta function. Thus, when reflections are scaled, time-shifted versions of the source signal, they are represented by delta functions in the cepstrum. This result suggests that, if the delta functions in the complex cepstrum at t_o intervals are removed, and the inverse cepstrum operations are performed, the recovered time history will be that of the original signal without the reflection.

In typical numerical experiments, reflections are not perfectly scaled, time-shifted versions of the source signal, but

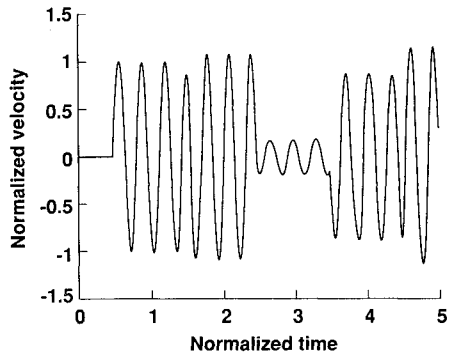

Fig. 2 Time series at duct midpoint.

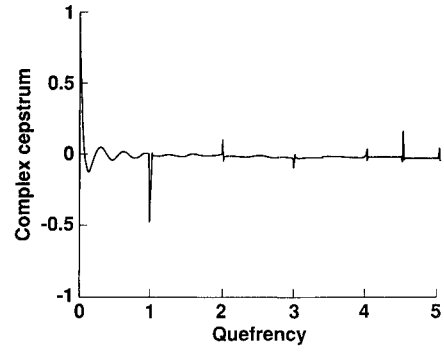

Fig. 3 Complex cepstrum of exponentially damped time series.

are distorted by boundary conditions or numerical errors. Thus, the reflections occur not as delta functions, but as peaks with diminished amplitude and broader width. It is simple to distinguish between the source signal and perfect reflections in the cepstrum, but this distinction becomes more difficult when the reflected signal is distorted. Therefore, in the work presented in this paper, hard-wall boundary conditions will be prescribed to reduce the distortion of the reflected signal.

Application of Cepstrum Theory

Consider plane sinusoidal wave propagation in a duct, as illustrated in Fig. 1. A sine wave is continuously being generated by a piston at $x = 0$. This wave travels down the duct and impinges upon the closed end at $x = l$ where it is reflected back into the duct and interacts with the waves being continuously generated at the piston. The velocity field $u(x, t)$ in the duct is analytically determined by solving the wave equation with the appropriate boundary and initial conditions:

$$\frac{\partial^2 u}{\partial t^2} = c_o^2 \frac{\partial^2 u}{\partial x^2} \qquad 0 < x < l, \quad 0 < t$$

$$u(0, t) = V_o \sin(\omega_o t) \qquad t > 0$$

$$u(l, t) = 0 \qquad t > 0 \tag{4a}$$

$$u(x, 0) = u_t(x, 0) = 0 \qquad 0 \le x \le l \tag{4b}$$

where c_o is the speed of sound, V_o the maximum amplitude of the disturbance, and ω_o the frequency of the disturbance. To determine the velocity field in the duct, the wave equation and boundary conditions are solved by using the Laplace transformation, and the solution in the time domain is found to be

$$u(x, t) = V_o \sum_{n=0}^{\infty} \{\sin[\omega_o \alpha_n] H[\alpha_n] - \sin[\omega_o \beta_n] H[\beta_n]\} \tag{5}$$

where

$$\alpha_n = t - \left(\frac{x + 2ln}{c_o}\right), \qquad \beta_n = t - \left(\frac{2l(1 + n) - x}{c_o}\right)$$

and the Heaviside function $H[t - t_o]$ is defined by

$$H[t - t_o] = \begin{cases} 1, & \text{if } t - t_o \ge 0 \\ 0, & \text{otherwise} \end{cases} \tag{6}$$

A graph of the velocity at the duct midpoint is presented in Fig. 2. Graphical results presented are normalized by the ambient speed of sound c_o and duct length l.

Note that the velocity in Fig. 2 is zero up to a normalized time of 0.5, the time for the sine wave to reach the duct midpoint. The velocity at the duct midpoint then oscillates sinusoidally with frequency ω_o and amplitude V_o until a nor-

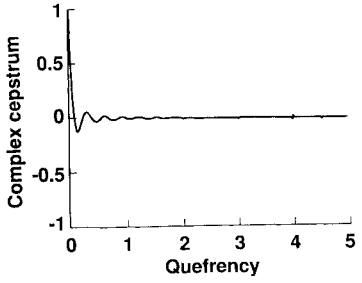

Fig. 4 Complex cepstrum of the exponentially damped time series—reflections removed.

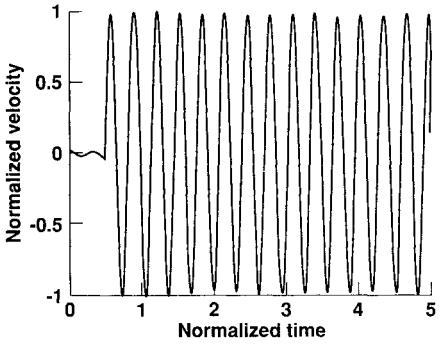

Fig. 5 Recovered source signal.

malized time of 1.5, the time it takes the wave to travel to the end of the duct, reflect, and return to the duct midpoint. After this time, the amplitude of the sine wave depends on the interactions of the sine waves being generated by the piston and the sine waves reflecting from the duct ends.

Using the definition of the complex cepstrum and applying it to the Fourier transform of the velocity field in the duct, the complex cepstrum is written as

$$C_c(x,\tau) = \int_{-\infty}^{\infty} \left(\mathcal{F}[S(\omega)e^{-i\omega x/c_o}] + \mathcal{F}\left[\frac{(1 - e^{-i2(l-x)\omega/c_o})}{(1 - e^{-2i\omega l/c_o})}\right]\right\} e^{i\omega\tau}\mathrm{d}\omega$$

$$= C_{co}(x,\tau) + \int_{-\infty}^{\infty} \{\mathcal{F}[(1 - e^{-i2(l-x)\omega/c_o})] - \mathcal{F}[(1 - e^{-2i\omega l/c_o})]\} e^{i\omega\tau}\mathrm{d}\omega \quad (7)$$

where C_{co} is the complex cepstrum of the source signal and the integral term contains the information that represents the undesired reflections in the time history due to the presence of the artificial boundary. Using the expansion of the logarithm, interchanging the order of integration and summation, and applying the definition of the Dirac delta function, Eqs. (7) become

$$C_c(x,\tau) = C_{co}(x,\tau) + 2\pi \sum_{n=1}^{\infty} \frac{(-1)^{n+1}}{n} \left\{ \delta\left[\tau - \frac{2ln}{c_o}\right] - \delta\left[\tau - \frac{2n(l-x)}{c_o}\right]\right\} \quad (8)$$

Thus, the complex cepstrum of the velocity in the duct is the linear combination of the complex cepstrum of the velocity field of the source signal and delta functions occurring at multiples of $[2(l - x)]/c_o$ and $2l/c_o$ and alternating in sign. Note that, because the distance between the boundary and the point of computation is known, the quefrencies that represent undesired reflections in the solution are also known. Thus, one may distinguish between reflections from real surfaces and artificial boundaries and remove only the information corresponding to the latter of the two. This result suggests that, if the delta functions in the complex cepstrum at $[2(l - x)]/c_o$ and $2l/c_o$ intervals are removed, and the inverse cepstrum operations are performed, the recovered time history will be that of the original signal without the reflection.

Complex Cepstrum Numerically Applied to Analytical Solution

The complex cepstrum is computed numerically with subroutines available from the Institute of Electrical and Electronics Engineers.[14] The time sequence of Fig. 2 is multiplied by a decaying exponential function and 512 zeroes are appended to minimize aliasing. Exponential weighting and appending zeroes are two processes known to improve the computation of the cepstrum and are discussed elsewhere.[4-13] The complex cepstrum is computed for the exponentially weighted time sequence, and the results are presented in Fig. 3. The smooth curve that oscillates at the source frequency ω_o and decays rapidly with quefrency is the portion of the complex cepstrum carrying the information about the source signal. The peaks in the cepstrum at quefrency multiples of $\tau = n$ correspond to the reflections in the original time sequence, as predicted by the theoretical result of Eq. (8). This figure shows how the information about the source sine wave is distributed over a fairly broad quefrency range.

Because the information corresponding to the source signal spans a wide quefrency range, the spikes in the cepstrum are removed by a comb liftering process described in the literature.[7-10] In the comb liftering process, only the information at the quefrencies corresponding to the delay time of reflections from the artificial boundaries are removed. The complex cepstrum of the exponentially weighted time series with reflections removed is illustrated in Fig. 4. This figure shows that more of the information about the source signal is maintained and most of the peaks corresponding to reflections in the time history are removed.

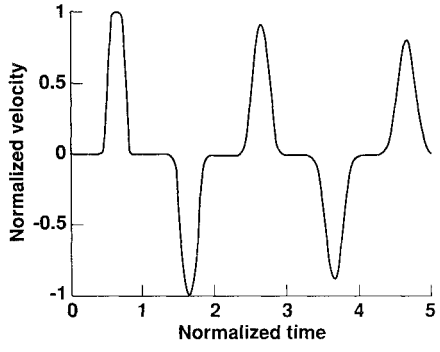

Fig. 6 Time history of duct midpoint.

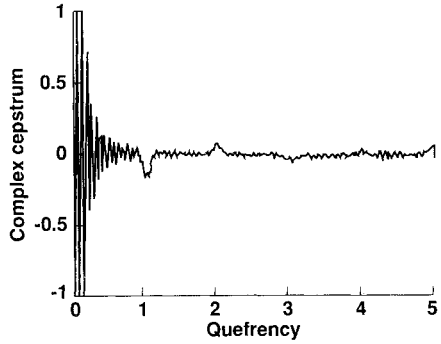

Fig. 7 Complex cepstrum of time history.

The inverse complex cepstrum corrected by multiplication of the inverse exponential function is presented in Fig. 5. The final result is accurate recovery of the source signal without the contamination of the reflections. To quantify the difference between the source signal and the inverse cepstrum, the mean squared error (MSE) is computed by the relation,

$$\text{MSE} = \frac{1}{N}\sum_{n=0}^{N-1}[s(n\Delta t) - \hat{s}(n\Delta t)]^2 \tag{9}$$

where n is the nth element of a discrete time sequence, $s(n\Delta t)$ the time history of the source signal in an infinite domain, $\hat{s}(n\Delta t)$ the inverse cepstrum of the source signal with reflections, and N the total number of points in the time history. The MSE is found to be 2.3×10^{-3}. Clearly, this error is small enough to be negligible in most cases.

Application of the Cepstrum to a One-Dimensional CFD Solution

A study of the application of the cepstrum technique to plane wave propagation in an infinite duct is presented in this section. The problem is modeled by solving the one-dimensional Euler equations in a closed-ended duct because the effects of the boundaries on the solution are to be removed by the complex cepstrum. The strategy is to apply the very simple hard-wall boundary condition and remove its effect on the solution by the complex cepstrum. Although this may seem unreasonable since the boundary is supposed to be nonreflecting, imposing hard-wall boundary conditions is simple and removing reflections from the cepstrum is easier when there is no distortion of the reflected information caused by nonreflecting boundary conditions.

The implicit upwind finite volume method is used to solve the Euler equations. The upwind algorithm used in this paper uses flux vector splitting and solves the Euler equations in conservation form, as outlined in Anderson et al.[15] The geometry of the modeled problem is identical to the one illustrated in Fig. 1, but the source at the left hand boundary is

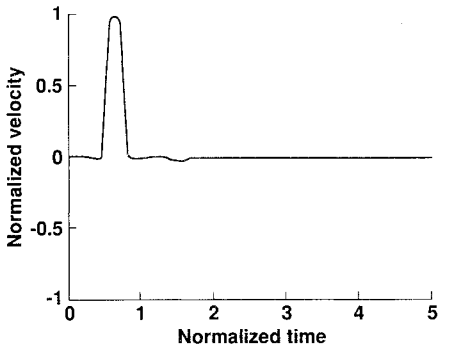

Fig. 8 Inverse cepstrum of time history—reflections removed.

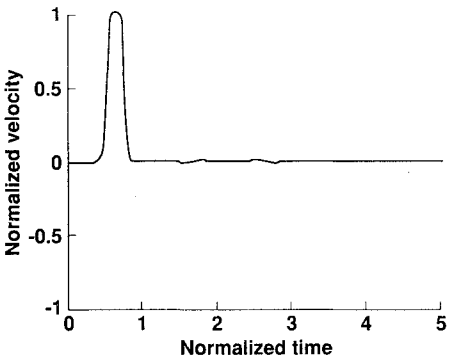

Fig. 9 Solution obtained by prescribing nonreflecting conditions.

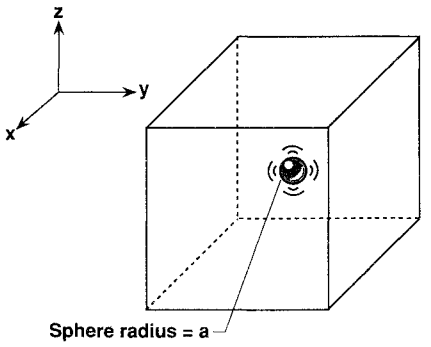

Fig. 10 Monopole source in a cubic computational domain.

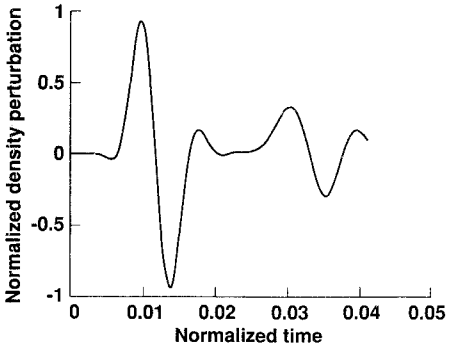

Fig. 11 Time history at a grid point midway between the source and wall boundary.

modeled as an impulse. The small impulsive disturbance to the flow is introduced to the initially quiescent duct at the boundary at $x = 0$. By characteristic theory, for subsonic flow there are two characteristic lines going into the flow domain at the left hand boundary. According to Kreiss,[16] this implies that two conditions are prescribed along this boundary and other flow variables are computed by the governing equations. Therefore, at the source boundary, two conditions are applied. In this example, the normalized speed of sound c_o is specified to be unity and the velocity of the source normalized by the sound velocity is given by

$$\bar{u}(0, t) = \begin{cases} A & \bar{t} < \bar{t}_s \\ 0 & \text{otherwise} \end{cases} \tag{10}$$

where A is a small amplitude with a numerical value of 1×10^{-6}, and $\bar{t}_s$ is the normalized pulse stop time taken to be 0.25. This small amplitude is chosen so that the results may be compared to linear theory. Characteristic theory states that there is one characteristic line going into the flow domain at the right hand boundary. For a hard-walled boundary condition, the condition prescribed is that $u(t) = 0$ for all t. All other flow variables are derived from the governing equations.

Figure 6 presents the time history of $\bar{u}/A$ at the duct midpoint. The solution is obtained using 501 grid points and a time step of 0.0018. This numerical result decays in time as a result of numerical damping. This damping is a benefit for application of the cepstrum method because it smooths the time history and broadens its spectrum. A better solution can be obtained by decreasing the time step or increasing the number of grid points in the solution.

The complex cepstrum of the time history is presented in Fig. 7. Note that the peaks in the cepstrum are not distinct for the solution obtained by the upwind method. The distortion in the reflected signals have broadened the peaks corresponding to reflections. This does not complicate the process of removing spikes in the cepstrum, however, because the normalized time it takes a wave to travel from the duct midpoint to the duct end and return is known.

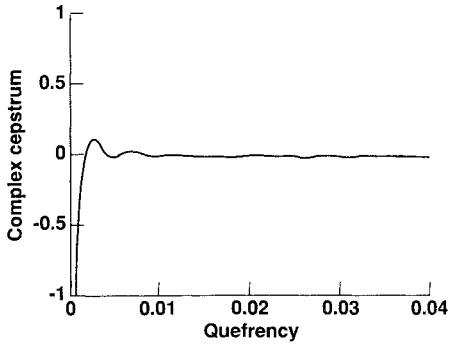

Fig. 12 Complex cepstrum of time history.

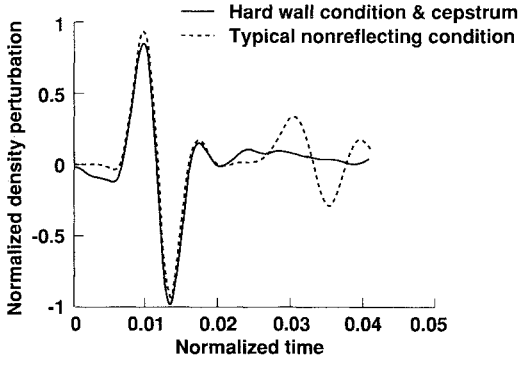

Fig. 13 Comparison of the inverse complex cepstrum with reflections removed and the results obtained by applying typical nonreflecting boundary conditions.

The peaks corresponding to reflections are removed from complex cepstrum by zeroing at all quefrencies < 0.7, and the resulting inverse complex cepstrum is illustrated in Fig. 8. Note that reflections have been removed from the CFD solution and the original is reproduced with little reflection. Although the solution contains evidence of one of the reflections, most reflection information is eliminated. Also note that the amplitude of the signal has been somewhat diminished because some information has been lost in the filtering process.

Although the theory requires that the reflected signal be a time shifted, scaled version of the original for the cepstrum method to be applied, these results show that, in practice, reasonable results may be obtained in spite of slight distortion caused by numerical methods.

The inverse complex cepstrum is compared to the upwind CFD solution where nonreflecting boundary conditions are applied. The exit boundary condition for this case is prescribed as suggested by Schmidt and Jameson.[17] The velocity is extrapolated in time,

$$u^n = 2u^{n-1} - u^{n-2} \tag{11a}$$

and the pressure is computed from the expression

$$p^n = p^{n-1} + \rho^{n-1}c_o^{n-1}(u^n - u^{n-1}) \tag{11b}$$

where the superscripts denote time level. The time history of this CFD solution is presented in Fig. 9. This figure shows that small reflections are still present in the solution, but the solution is at least as good as that obtained by applying the cepstrum to the upwind solution. In the one-dimensional case, then, it is difficult to justify the use of the complex cepstrum because good results are achieved by prescribing nonreflecting boundary conditions, which are possible because all waves are normally incident on the boundary. However, general nonreflecting conditions are not available for multidimensional flows. The application of the complex cepstrum to a three-dimensional solution is the topic of the next section.

Application of the Cepstrum to a Three-Dimensional CFD Solution

The next example of application of the complex cepstrum method to CFD solutions shows the utility of the method in multidimensional problems. A monopole source in infinite space is modeled on the computer as a point source in a cubic region of numerical space, as illustrated in Fig. 10. The conditions prescribed on the boundaries of the numerical domain are hard-wall conditions in which the velocity normal to the boundary is zero. This boundary condition is simple to prescribe, but will act as a surface and reflect the waves generated at the monopole source back into the computational solution domain. The cepstrum is used to remove the spurious reflections from the solution. The Euler equations are solved in three-dimensional space with CFL3D, an upwind finite volume computer program developed at NASA Langley Research Center,[18] which solves the time-dependent conservation law form of the Euler equations in generalized coordinates. The interested reader is referred to Thomas et al.[18] and Anderson et al.[19] for details on the algorithm.

The problem is modeled as follows. A single source is located in the center of a cube with edge lengths of 10 m. The system is made dimensionless with a length equal to the distance a sound wave in air travels in 1 s (343 m), the velocity of sound in air (taken to be 343 m/s), and the ambient density of the medium (taken to be 1.14 kg/m^3). A cubic grid is created with 34 grid points in each direction. In order to resolve the discontinuities of the expected N wave, many more grid points are required. However, the associated computational cost of a finer grid was prohibitive and not believed necessary for the purposes of this paper. All six boundary planes are prescribed as hard-wall boundaries. The initially quiescent computational domain is perturbed as mass is introduced to the center cell of the cubic volume,

$$\bar{\rho}_c = \begin{cases} \bar{\rho}_o + A & 0 < \bar{t} < \bar{t}_s \\ \bar{\rho}_o & \bar{t} > \bar{t}_s \end{cases} \tag{12}$$

where $\bar{\rho}_c$ is the normalized density at the center cell volume, $\bar{\rho}_o$ the normalized ambient density (which is 1), $\bar{t}_s$ the small normalized time of 0.003, and A the amplitude of the density perturbation, which is chosen to be a small value $A = 1 \times 10^{-3}$. The solution is advanced with a time step of 8×10^{-5}. The normalized pressure at the monopole surface is given by $\bar{p}_c = \bar{\rho}_c/\gamma$ since the normalized sound speed is 1. Thus, the sound pressure level (SPL) of the source is given by

$$\text{SPL} = 20 \log \frac{\bar{p}_c\, p_{\text{atm}}}{p_{\text{ref}}} = 128 \text{ dB} \tag{13}$$

where the normalized pressure at the source has been dimensionalized by the atmospheric pressure so that the standard reference pressure for air $p_{\text{ref}} = 28$ μPa could be used in the calculation.

Although results are obtained for each grid point in the solution, only results at one location are presented here. Figure 11 shows the time history of the density perturbation at a grid point approximately midway between the source and one of the boundary planes. The features of the compression and expansion are smoothed out as a result of numerical dissipation. The dissipation could have been minimized with a finer grid since numerical error is a function of the spatial and temporal resolution, but the memory requirements for a finer grid were prohibitive. The wave amplitude drops off rapidly in time because of numerical dissipation and spreading losses. The reflected wave is a scaled, somewhat distorted, time shifted version of the original. Because the reflected

wave is a result of a spherical wave bouncing off a set of plane hard-wall boundaries, the reflected wave is not spherical.

Figure 12 shows the complex cepstrum of the time history of Fig. 11. The spikes in the cepstrum are not distinguished easily from the cepstrum of the source signal, but they are removed by zeroing the cepstrum of all quefrencies > 0.018. The heavy line in Fig. 13 shows the inverse cepstrum of the time sequence with the reflection removed. The reflection has been nearly completely eliminated, although some small oscillations still distort the time sequence. Some error would be expected, however, because of the distortion in the reflected signal. The cepstrum method appears to be applicable to wave solutions when the reflected wave is distorted by the algorithm and boundary conditions.

To compare the results to solutions obtained by prescribing typical nonreflecting boundary conditions, CFL3D is run with its standard extrapolation and inflow-outflow boundary conditions. The results obtained for these two types of boundary conditions are very similar, and so only the results from the inflow-outflow boundary condition are presented with the dashed line in Fig. 13. The results from this typical nonreflecting boundary condition case cannot be distinguished from those obtained from the hard-wall condition, illustrating that the nonreflecting conditions are reflecting information back into the computational domain. Clearly, the results provided by removing the reflections with the complex cepstrum are far better than the results obtained by applying nonreflecting boundary conditions. In fairness to the authors of CFL3D, the standard boundary conditions available in the code are developed primarily for use with steady problems, and the code has the flexibility for users to incorporate specialized boundary conditions. But the point that must be reiterated here is that local, perfectly nonreflecting boundary conditions for unsteady, multidimensional flows are not thought possible. Hence, using the cepstrum method as a postprocessor to remove spurious reflections is a potential remedy to this difficult problem.

Concluding Remarks

It was shown that the complex cepstrum may be used to remove spurious reflections introduced by artificial boundary conditions in CFD solutions. The results obtained by applying the complex cepstrum to a three-dimensional CFD solution were superior to those obtained by imposing typical nonreflecting boundary conditions. Thus, the complex cepstrum provides an alternative to the difficult task of developing nonreflecting boundary conditions. Further research is required before the complex cepstrum may be used routinely in conjunction with CFD calculations. The limitations of applying the method to solutions where the reflected signal is severely distorted by long-time CFD solutions or nonreflecting boundary conditions needs to be determined, and development of more efficient techniques for applying the complex cepstrum analysis procedure to CFD computations is required. Future work will focus on the application of the complex cepstrum internal to CFD computations, rather than as a postprocessor to CFD solutions. The present work shows that the cepstrum method may be applied to CFD solutions; it is quite possible that other digital signal processing tools may also prove to be useful to the numerical experimentalist.

References

[1]Acton, E., and Cargill, A. M., "Non-Reflecting Boundary Conditions for Computations of Unsteady Flows in Turbomachines," *Proceedings of the Fourth International Symposium on Unsteady Aerodynamics and Aeroelasticity of Turbomachines and Propellers*, edited by H. L. Gullus and S. Servaty, Aachen, Germany, 1985, pp. 211–228.

[2]Hedstrom, G. W., "Non-Reflecting Boundary Conditions for Nonlinear Hyperbolic Systems," *Journal of Computational Physics*, Vol. 30, 1979, pp. 222–237.

[3]Watson, W., and Myers, M., "Time-Dependent Inflow-Outflow Boundary Conditions for 2-D Acoustic Systems," AIAA Paper 89-1041, San Antonio, TX, April 1989.

[4]Bogert, B., Healy, M., and Tukey, J., "The Quefrency Alanysis of Time Series for Echoes: Cepstrum Pseudo-Autocovariance and Saphe Cracking," *Proceedings of Symposium on Time Series Analysis*, edited by M. Rosenblatt, Wiley, New York, 1963, pp. 209–243.

[5]Oppenheim, A. V., Schafer, R. W., and Stockham, T. G., Jr., "Nonlinear Filtering of Multiplied and Convolved Signals," *Proceedings of the IEEE*, Vol. 56, No. 8, 1968.

[6]Childers, D. G., Skinner, D. P., and Kererait, R. C., "The Cepstrum: A Guide to Processing," *Proceedings of the IEEE*, Vol. 65, No. 10, 1977, pp. 1428–1443.

[7]Perraud, J. C., "Theory and Methodology of Cepstral Analysis," M.S. Thesis, University of Southampton, 1979.

[8]Peardon, L. G., "Aspects of Cepstral Analysis and Epoch Detection," Council for the National Academic Awards Master of Philosophy Thesis, Aug. 1979.

[9]Tavakolli, S., "Application of the Cepstrum Technique to Location of Acoustic Sources in the Presence of a Reflective Surface," M.S. Thesis, Virginia Polytechnic Institute and State University, Blacksburg, VA, Dec. 1986.

[10]Meadows, K. R., "Cepstrum Analysis and Applications to Computational Fluid Dynamic Solutions," M.S. Thesis, George Washington Univ., Washington, DC, April 1990.

[11]Tribolet, J. M., "A New Phase Unwrapping Algorithm," *IEEE Transactions on Acoustics, Speech, and Signal Processing*, Vol. ASSP-25, No. 3, 1977, pp. 170–177.

[12]Hassab, J. C., and Boucher, R., "Analysis of Signal Extraction, Echo Detection, and Removal by the Complex Cepstrum in Presence of Distortion and Noise," *Journal of Sound and Vibration*, Vol. 40, 1975, pp. 321–335.

[13]Hammond, J. K., and Peardon, L. G., "Cepstral Analysis and Applications," Lecture Notes. I.S.V.R., University of Southampton, 1985.

[14]*Programs for Digital Signal Processing*, Digital Signal Processing Committee, IEEE Acoustics, Speech, and Signal Processing Society (ed.), Institute of Electrical and Electronics Engineers, New York, 1979.

[15]Anderson, W. K., Thomas, J. L., and van Leer, B., "A Comparison of Finite Volume Flux Vector Splittings for the Euler Equations," *AIAA Journal*, Vol. 24, No. 9, 1986, pp. 1453–1460.

[16]Kreiss, H. O., "Initial Boundary Value Problems for Hyperbolic Systems," *Communications of Pure and Applied Mathematics*, Vol. 1, 1970, pp. 277–298.

[17]Schmidt, W., and Jameson, A., "Recent Developments in Finite-Volume Time-Dependent Techniques for Two and Three Dimensional Transonic Flows," Von Karman Institute for Fluid Dynamics Lecture Series 1982-04, Computational Fluid Dynamics, March 29–April 2, 1982.

[18]Thomas, J. L., Krist, S. T., and Anderson, W. K., "Navier Stokes Computations of Vortical Flows over Low Aspect Ratio Wings," *AIAA Journal*, Vol. 28, No. 2, 1990, pp. 205–212.

[19]Anderson, W. K., Thomas, J. L., and Whitfield, D. L. "Three-Dimensional Multigrid Algorithms for the Flux Split Euler Equations," NASA TP-2829, Nov. 1988.